

Pulsed EPR and ENDOR Investigation of Hydrogen Atoms in Silsesquioxane Cages

N. Weiden¹, M. Päch², and K.-P. Dinse¹

¹Physical Chemistry III, Technical University Darmstadt, Darmstadt, Germany

²Radiation Laboratory, University of Notre Dame, Notre Dame, Indiana, USA

Received June 25, 2001

Abstract. High sensitivity and spectral resolution provided by pulsed electron paramagnetic resonance and electron nuclear double resonance techniques at high Larmor frequencies open the way for a study of atoms in chemical traps. As an example we studied deuterium atoms encased in silsesquioxane cages to probe the cage symmetry as function of temperature. An analysis of the temperature dependence showed that the system undergoes a structural phase transition near 100 K. At this temperature the character of distortion of the ideal cubic symmetry changes from oblate to prolate (or vice versa). With quantum chemical methods, a model for cage escape of the encased atom could be derived. The calculated escape barrier of 0.9 eV is close to the experimental value derived by thermal release experiments. Although the encased deuterium atom exhibits an isotropic hyperfine coupling constant nearly identical with the free atom value, a spin population analysis revealed that approximately 10% of the spin density is transferred to the cage. We therefore conclude that confinement of the hydrogen atom leads to a compression of its wave function compensating the decrease of spin density. In this respect the system falls somewhat short of the properties of an ideal cage, being defined by well decoupled atomic and molecular wave functions.

1 Introduction

The study of individual atoms or molecules is one of the challenging problems in spectroscopy. The inherent high sensitivity of optical spectroscopy has led to amazing progress in the field of spectroscopy of single species which can either be studied “in vacuum” or embedded in a solid matrix. In the latter case, decoupling from perturbing influences of the surrounding is a major issue but spectral shifts resulting from solute-solvent interactions could actually be used to frequency select single species. It is one of the current problems to relate spectroscopic parameters like frequency shifts of optical transitions to specific host-guest interactions. Even without specific models for this interaction, the effect can be used to sense structural changes in the surroundings.

Alternatively, the preparation of a large set of nearly isolated and – as a result – identical species suspended in a solid matrix would open the way for the application of the less sensitive magnetic resonance technique. In our studies we therefore concentrate on this aspect and investigate systems for which optimal guest isolation can be achieved in solids or even in liquids at room temperature. As was shown previously, highly reactive atoms like nitrogen or phosphorous could be stabilized in fullerenes acting as inert chemical traps, and more recently even highly charged molecular clusters like Sc_3N^{6+} have been encapsulated in C_{80} . Unfortunately, hydrogen atoms could not be encased and observed on a sufficiently long time scale in fullerenes, a model system being expected to be analyzed easier with respect to the influence of confinement on atomic wave functions.

As alternative to the pure carbon cages, we used silsesquioxane to stabilize hydrogen inside its cubic environment. These compounds were shown earlier to be able to confine hydrogen atoms on a time scale of months at room temperature [1]. Applying the high-resolution and high-sensitivity technique of pulsed electron nuclear double resonance (ENDOR) at high frequencies (95 GHz electron Larmor frequency) we invoked deuterium nuclear spins to determine possible cage deformations and the amount of spin transfer from the encased atom to the cage. The analysis of the temperature dependence of electron spin relaxation rates should help to identify the dominant interaction mechanism of the paramagnetic compound with the matrix.

2 Experimental

Samples of H or D encased in $\text{Si}_8\text{O}_{12}(\text{CH}_2\text{CH}_3)_8$ ($\text{Si}_8\text{O}_{12}\text{Et}_8$) have been prepared by γ irradiation with a ^{60}Co source as described elsewhere [2]. Samples recrystallized from ethanol were studied without further purification. All spectra were taken with a commercial W-band electron paramagnetic resonance (EPR) spectrometer (Bruker E680) equipped with a homebuilt ENDOR probe head [3]. Radio-frequency (rf) power of up to 1 kW was obtained with a pulsed amplifier (Dressler).

3 Results and Discussion

In $\text{Si}_8\text{O}_{12}\text{Et}_8$, the proton hyperfine coupling constant (hfcc) had been determined at room temperature as $a(\text{H}) = 1413$ MHz, very close to the free atom value of 1420.406 MHz [4]. This large value would lead to ENDOR transitions at about 550 and 850 MHz in an external field of 3.4 T, well outside the working range of our ENDOR probe head. For this reason, all experiments were performed with deuterium as nuclear spin probe instead, for which ENDOR transitions in W-band are shifted to about 88 and 131 MHz. Deuteron nuclei have the additional advantage that electric field gradients, if present, can be sensed with their electric quadrupole moment.

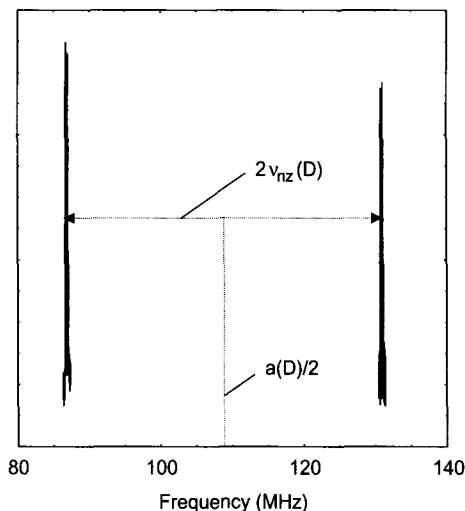


Fig. 1. Deuteron ENDOR of polycrystalline $\text{D@Si}_8\text{O}_{12}\text{Et}_8$ observed at 130 K in an external field of 3.4 T.

In Fig. 1, an ENDOR spectrum is displayed, showing two deuteron transitions, separated by twice the nuclear Larmor frequency and centered at $a(\text{D})/2$. The observed solutionlike ENDOR spectrum indicates that second-rank tensor interactions are small. When exciting the central hf component of the three-line EPR spectrum, higher spectral resolution reveals a splitting of the 87 MHz structure in a line doublet (see Fig. 2). A similar doublet is observed around 131 MHz. In total, four instead of two ENDOR lines are observed, because the frequency degeneracy of ENDOR transitions is lifted, which connect $m_I = +1, 0$ and $m_I = 0, -1$ nuclear spin sublevels in the $m_S = +1/2$ and $-1/2$ electron spin states. By selective microwave excitation of either $m_I = +1$ or -1 EPR transition instead of the central EPR hf component, a single ENDOR transition and no doublet is detected. In sufficient accuracy the line separation of 240 kHz is calculated by considering hyperfine interaction (hfi) in second-order perturbation theory. Only because of very small powder line broadening (near absence of hfi anisotropy in our system) in combination with a large hfcc can this second-order splitting be resolved in a solid even in W-band.

In Fig. 2, no line asymmetry is detected which would be indicative of anisotropic hfi (dipolar or quadrupolar). As was discussed in detail in ref. 3, comparing powder line shapes of ENDOR transitions originating from transitions within a specific electron spin level allows separation of line shape contributions from dipolar and quadrupolar interactions. This is possible because dipolar and quadrupolar hfi depends linearly or quadratically on m_I , respectively. In the first order, allowed ENDOR transitions ($\Delta m_I = \pm 1$) in the $m_S = +1/2$ and $-1/2$ sublevels are expected at

$$\begin{aligned} \nu_{(m_I=+1, m_I'=0)} &= \left| \left(\pm \frac{1}{2} A_{zz} + \frac{3}{2} Q_{zz} \right) \frac{1}{2} (3 \cos^2 \Theta - 1) \pm \frac{1}{2} a_{\text{iso}} - \nu_n \right|, \\ \nu_{(m_I=-1, m_I'=0)} &= \left| \left(\pm \frac{1}{2} A_{zz} - \frac{3}{2} Q_{zz} \right) \frac{1}{2} (3 \cos^2 \Theta - 1) \pm \frac{1}{2} a_{\text{iso}} - \nu_n \right| \end{aligned} \quad (1)$$

the choice of sign depending on the m_S value [3]. In the usual fashion, ν_n denotes nuclear Larmor frequency, m_I describes nuclear spin magnetic quantum number, a_{iso} denotes the isotropic deuteron hfcc, $A_{zz}(\Theta, \Phi)$ and $Q_{zz}(\Theta, \Phi)$ are (z, z) -elements of the traceless dipolar and quadrupolar hyperfine tensors (defined by **SAI** and **IQI**, respectively) after transformation to the laboratory frame. In its eigenframe, Q_{zz} can be related to the nuclear quadrupole coupling constant eQq/h by $Q_{zz} = eQq/2h$ in case of ^2H with $I = 1$. Equation (1) is valid in the first-order perturbation theory. The small spectral shift due to nonsecular terms of **A** leads to line separation as discussed above but will not affect the line shape analysis.

If selective microwave excitation of a particular hf component is possible for a pulsed ENDOR experiment, either the sum or difference of both terms will contribute to the ENDOR powder line shape. Under conditions when the second-order splitting prevails, microwave excitation of the central $m_I = 0$ hf component allows direct comparison of both ENDOR lines (special case of a single $I = 1$ nuclear spin). Thus one can avoid any complications which might other-

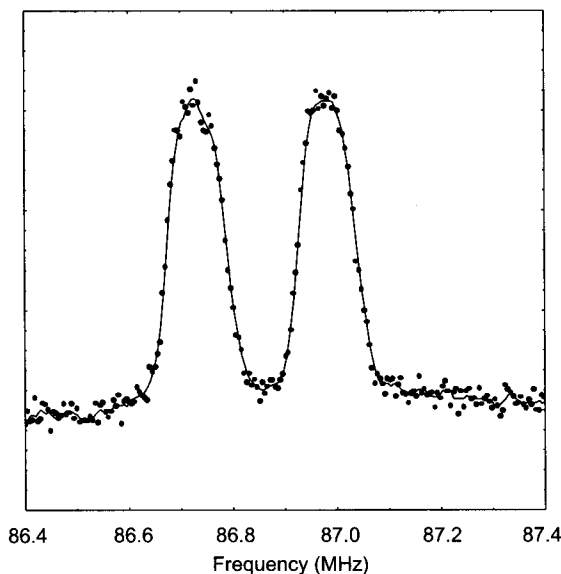


Fig. 2. ENDOR lines detected at 130 K originating from transitions within the $m_S = +1/2$ electron spin manifold.

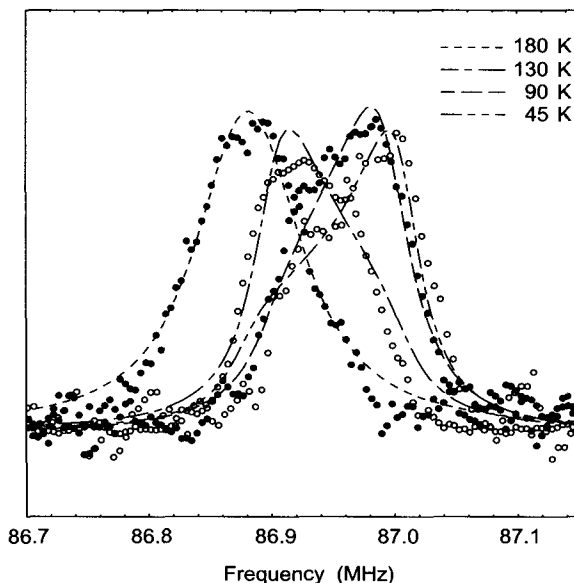


Fig. 3. Low-frequency ENDOR transitions of $\text{D@Si}_8\text{O}_{12}\text{Et}_8$ at different temperatures. The experimental spectra are fitted assuming powder broadening originating from hfi of axial symmetry.

wise result from the change of the external field, necessary to switch between related ENDOR transitions. Identical line shapes of ENDOR transitions as seen in Fig. 2 thus indicate insignificant quadrupole interaction. The line width of approximately 100 kHz is presumably due to a small variation of the spin density at the nucleus, i.e., a variation of the isotropic hfcc.

In the temperature range of 45 to 130 K, however, high-resolution ENDOR reveals that the lines can no longer be simulated with a simple symmetric Gaussian or Lorentzian line profile but rather exhibit some asymmetry, as is shown in Fig. 3. In order to achieve the necessary resolution, a Davies pulse sequence with rf pulses between 70 and 120 μs duration optimized with respect to electronic relaxation time was used. If interpreted as arising from an axially symmetric hfi, the sign of the principal component of this tensor changes in this temperature range. Such sign inversion would be indicative of a gradual deformation of the cage from prolate to oblate or vice versa. Such an interpretation is in line with previous conclusions derived from an analysis of the temperature dependence of X-ray data, by which deformations of the cube were also deduced. The deformation was attributed to thermal activation of symmetry-breaking cage modes [5]. At higher temperatures (180 K and above), no more deviation from cubic symmetry can be detected by ENDOR. It should be noted that ENDOR experiments in the critical transition temperature range in which T_{2e} dropped below 1 μs were only possible because reasonably long T_{1e} allowed the application of sufficiently long rf pulses.

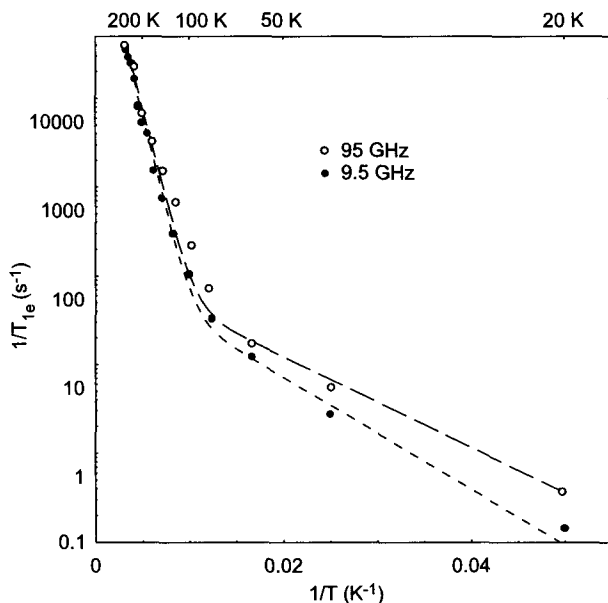


Fig. 4. Electron spin-lattice relaxation rate as function of temperature measured at 9.5 and 95 GHz, respectively. The temperature dependence of both data sets can be described by two activation energies of approximately 150 and 1000 K.

The postulated change in time-averaged cage symmetry should also be correlated with a change in the spectral density function of fluctuations sensed by the encased atom. In Fig. 4, a plot of the electronic spin-lattice relaxation rate T_{1e}^{-1} shows that two different processes might be present, distinguished by their activation energies. Above 100 K, relaxation driven by the process with higher activation energy starts to dominate. At the same temperature, which according to our line shape analysis marks the transition from prolate to oblate average symmetry, T_{2e} is reduced significantly (see Fig. 5). The minimum value of about 0.5 μ s is observed at 80 K, close to the value (0.87 μ s, $T = 77$ K) reported earlier by Sasamori et al. [1]. It should be noted, however, that we observe a much longer spin relaxation time T_{1e} at nitrogen temperature (30 ms, this experiment; 13 μ s [1]). This discrepancy might originate from additional paramagnetic impurities presumably present in the earlier sample. Within measurement error, T_{2e} is independent of the external field, whereas T_{1e}^{-1} increases by approximately a factor of 2 at the higher field. This field independence is not surprising considering the near cubic symmetry at the hydrogen site. Only at the lowest temperatures, an increase of T_{2e} up to 12 μ s is observed in W-band, a value which is still small when considering that we investigate a dilute paramagnetic spin system in a deuterated matrix, in which nuclear spin diffusion is also inhibited. We therefore have to conclude that at 5 K the rigid limit has not been reached. All relaxation data depicted have been determined for encased hydrogen atoms. At 95

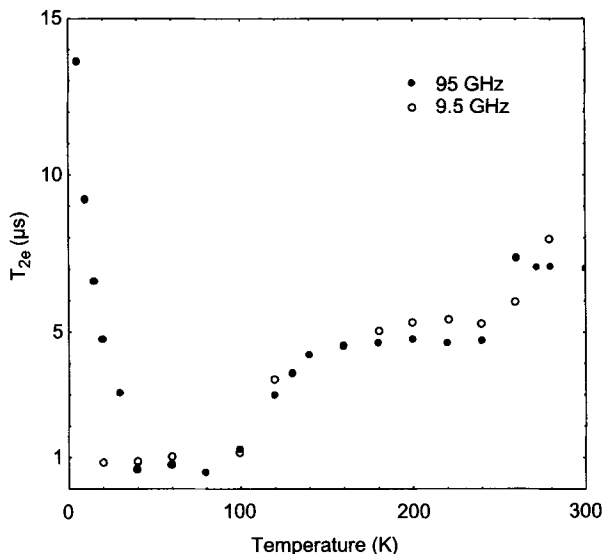


Fig. 5. Electron spin dephasing time T_{2e} as function of temperature. Data were taken for encased hydrogen atoms. No noticeable change was observed when investigating deuteron atoms instead.

GHz, no nuclear spin dependence could be observed for T_{2e} over the full temperature range. At a small number of temperature values this independence was also verified for T_{1e} .

The shift of the line center (see Fig. 3) can be used to determine accurate values for the change of the isotropic hfcc with temperature. Limited in accuracy only by the line width of the ENDOR transitions (and their signal-to-noise ratio), relative changes of $a(D)$ could be measured with error margins of less than 10^{-4} even at low temperatures. Such accuracy is difficult to obtain in EPR, because anisotropic contributions to the line shape as well as line shape distortions resulting from saturation inhibit an exact determination of line centers. High accuracy is necessary, however, for an evaluation of the generally small temperature-dependent shift originating from thermal population of vibrations of the encased atom. In this model, in which $a_{iso}(T)$ is assumed to be proportional to the occupation of eigenstates of a three-dimensional frequency-degenerate harmonic oscillator, the temperature dependence is calculated as [6]

$$\begin{aligned}
 a_{iso}(T) &= a_{iso}(0) + \Delta a \frac{\sum_{n=0}^{\infty} (n+1)(n+1/2)(n+3/2) \exp(-n\hbar\omega_0/k_B T)}{\sum_{n=0}^{\infty} (n+1)(n+1/2) \exp(-n\hbar\omega_0/k_B T)} \\
 &= a_{iso}(0) + \Delta a \frac{1 + \exp(-\hbar\omega_0/k_B T)}{1 - \exp(-\hbar\omega_0/k_B T)}, \quad (2)
 \end{aligned}$$

with a single relevant fit parameter ω for the vibrational mode. For a determination of ω it is sufficient to determine the transition from the constant low temperature behavior to the linear regime. As is shown in Fig. 6, the observed shift can be well described with this model. Because of the high accuracy of the data, only four experimental values determined in the relevant temperature range were sufficient for the analysis and as a result we obtain $\hbar\omega = 45.7$ meV, very close to the theoretical value of 38 meV, estimated from the approximated cage potential (see below).

With the Gaussian98W program package, the hydrogen escape barrier was studied. Along an exit path through the center of a cube face, the potential barrier was calculated as $\Delta E_a = 0.9$ eV. This value was obtained with the 6-31 G basis set and unrestricted B3LYP DFT parametrization and allowing for fully relaxed nuclear coordinates. In Fig. 7 the calculated potential is depicted. This calculated value is very close to the experimental value of $\Delta E_a^{\text{exp}} = 1.1$ eV, deduced from thermal release experiments [7]. Confirming the analysis from an earlier X-ray study, in our theoretical study only oxygen atoms are easily displaced, while the structure of silicon-centered tetrahedra is conserved [8]. With a harmonic approximation for displacement from the cage center as indicated in Fig. 7, the energy of the vibrational mode of the encased atom can be estimated as 38 meV for the deuterium atom.

Part of the theoretical study was also the question, to which extent the spin density is delocalized from the encased hydrogen atom in its doublet spin ground state to the cage nuclei. From previous EPR experiments performed in solution it was known that ^{29}Si nuclei exhibited nonzero isotropic hfcc, indicative of substantial spin transfer. The experimental value of $a_{\text{iso}}(^{29}\text{Si}) = 4.5$ MHz ($R = \text{CH}_3$)

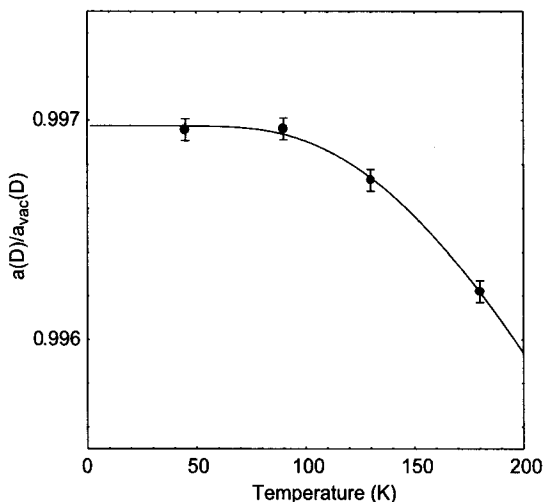


Fig. 6. Temperature dependence of ENDOR-derived deuteron hfcc, scaled with respect to the vacuum value. The solid line represents a fit assuming a fundamental deuterium vibrational mode of 45.7 meV.

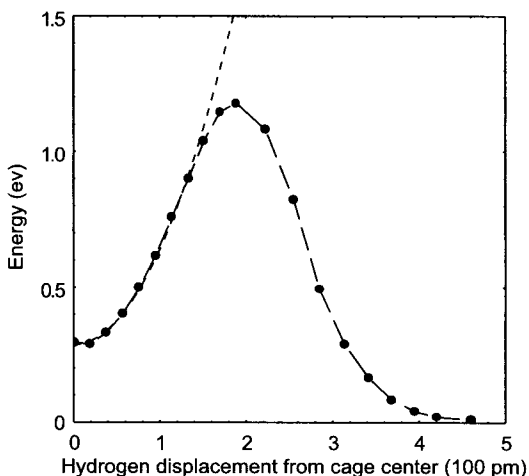


Fig. 7. Hydrogen escape potential calculated at the UB3LYP/6-31G level. Fully relaxed coordinates are assumed for each displacement step. The dashed line shows approximation of the cage potential by a harmonic potential.

could be quite well reproduced by our calculations ($a_{\text{calc}}(^{29}\text{Si}) = -5.11$ MHz; UB3LYP/6-31++G**). A spin population analysis of the optimized wave function showed that 10% spin density is actually transferred, nearly an order of magnitude more than in the much better decoupled N@C_{60} cage system. Judging from the size of the hydrogen hfcc, the expected 10% decrease of spin density apparently is compensated by an increase of electron spin density at the nucleus also by about 10%, resulting from spatial confinement of the hydrogen 1s function. This moderate increase can be compared with a nearly 50% increase of ^{14}N hfi originating from confinement in C_{60} with its “inert” inner surface [9].

Acknowledgements

Financial support from the Deutsche Forschungsgemeinschaft (Di182/22-2) is gratefully acknowledged. We are grateful to Prof. E. Roduner for sending us a copy of the Diploma Thesis of Barbara Gross.

References

1. Sasamori R., Okaue Y., Isobe T., Matsuda Y.: *Science* **265**, 1691 (1994)
2. Päch M., Stösser R.: *J. Phys. Chem. A* **101**, 8360 (1997)
3. Weiden N., Goedde B., Käß H., Dinse K.-P., Rohrer M.: *Phys. Rev. Lett.* **85**, 1544 (2000)
4. Anderson L.W., Pipkin F.M., Baird J.C. Jr.: *Phys. Rev. Lett.* **4**, 69 (1960)
5. Törnroos K.W.: *Acta Crystallogr. C* **50** 1646 (1994)
6. Dilger H., Roduner E., Scheuermann R., Major J., Schefzik M., Stößer R., Päch M., Fleming D.G.: *Physica* **288–290**, 482 (2000)

7. Päch M.: Ph.D. Thesis, Technical University Berlin, Berlin, Germany 1997.
8. Bieniok A.M., Bürgi H.-B.: J. Phys. Chem. **98**, 10735 (1994)
9. Almeida Murphy T., Pawlik T., Weidinger A., Höhne M., Alcalá R., Spaeth J.-M.: Phys. Rev. Lett. **77**, 1075 (1996)

Authors' address: Klaus-Peter Dinse, Physical Chemistry III, Technical University Darmstadt, Petersenstrasse 20, D-64287 Darmstadt, Germany